arXiv:2105.05636v3 [cs.CV] 5 Jan 2023

VL-NMS: Breaking Proposal Bottlenecks in Two-Stage Visual-Language Matching

CHENCHI ZHANG*, Zhejiang University, China
WENBO MA*, Zhejiang University, China
JUN XIAO, Zhejiang University, China
HANWANG ZHANG, Nanyang Technological University, Singapore
JIAN SHAO, Zhejiang University, China
YUETING ZHUANG, Zhejiang University, China
LONG CHEN†, Hong Kong University of Science and Technology, China

The prevailing framework for matching multimodal inputs is based on a two-stage process: 1) detecting proposals with an object detector and 2) matching text queries with proposals. Existing two-stage solutions mostly focus on the matching step. In this paper, we argue that these methods overlook an obvious *mismatch* between the roles of proposals in the two stages: they generate proposals solely based on the detection confidence (*i.e.*, query-agnostic), hoping that the proposals contain all instances mentioned in the text query (*i.e.*, query-aware). Due to this mismatch, chances are that proposals relevant to the text query are suppressed during the filtering process, which in turn bounds the matching performance. To this end, we propose VL-NMS, which is the first method to yield query-aware proposals at the first stage. VL-NMS regards all mentioned instances as critical objects, and introduces a lightweight module to predict a score for aligning each proposal with a critical object. These scores can guide the NMS operation to filter out proposals irrelevant to the text query, increasing the recall of critical objects, and resulting in a significantly improved matching performance. Since VL-NMS is agnostic to the matching step, it can be easily integrated into any state-of-the-art two-stage matching method. We validate the effectiveness of VL-NMS on three multimodal matching tasks, namely referring expression grounding, phrase grounding, and image-text matching. Extensive ablation studies on several baselines and benchmarks consistently demonstrate the superiority of VL-NMS.

CCS Concepts: • **Computing methodologies** → **Artificial intelligence**; *Natural language processing*; *Computer vision.*

Additional Key Words and Phrases: Text-guided Region Proposal Generation, Visual Grounding, Image-Text Matching, Non-Maximum Suppression

1 INTRODUCTION

Recently, visual-language tasks which require joint reasoning over both vision and natural language modalities have attracted great interest in the multimedia community. Matching multimodal inputs is one of the most fundamental abilities that can facilitate many high-level visual-language tasks. Considering different granularities of matching, there are two types of tasks: 1) **Instance-level matching**, where each text query refers to one targeted instance (referent) in the image and is explicitly grounded to one image region, *e.g.*, referring expression grounding (REG) [45, 48, 85] or phrase grounding (PG) [89]. 2) **Image-level matching**, where text queries describe the whole image and are matched with images holistically, *e.g.*, image-text matching (ITM) [7, 38, 44]. Both

*Both authors contributed equally to this research.
†Long Chen is the corresponding author.

Authors' addresses: Chenchi Zhang, chenchiz@zju.edu.cn, Zhejiang University, Hangzhou, Zhejiang, China, 310027; Wenbo Ma, mwb@zju.edu.cn, Zhejiang University, Hangzhou, Zhejiang, China, 310027; Jun Xiao, junx@zju.edu.cn, Zhejiang University, Hangzhou, Zhejiang, China, 310027; Hanwang Zhang, hanwangzhang@ntu.edu.sg, Nanyang Technological University, Singapore, 639798, Singapore; Jian Shao, jshao@cs.zju.edu.cn, Zhejiang University, Hangzhou, Zhejiang, China, 310027; Yueting Zhuang, yzhuang@zju.edu.cn, Zhejiang University, Hangzhou, Zhejiang, China, 310027; Long Chen, zjuchenlong@gmail.com, Hong Kong University of Science and Technology, Hong Kong, China, 999077.

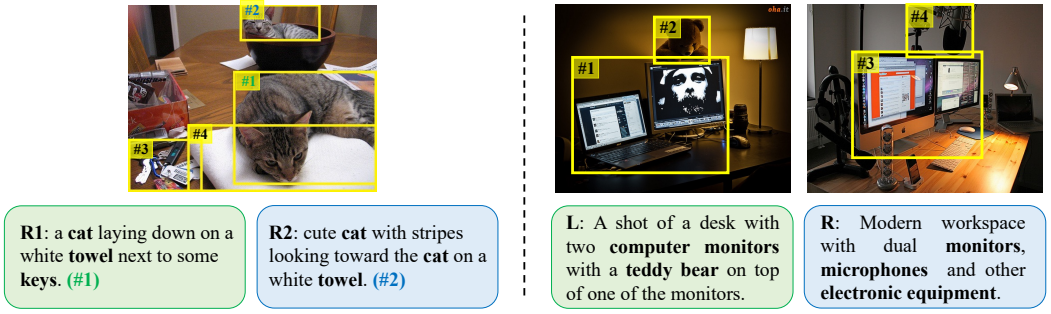

(a) An example of confusing referring expression. **(b)** An example of confusing image-sentence pair.

Fig. 1. Confusing examples from REG and ITM tasks. (a): A referring expression comprehension example from RefCOCOg [51]. Two similar expressions (R1 and R2) refer to different objects. (b): An image-text matching example from MSCOCO [43]. Two similar images with overlapping visual content.

two types of visual-language matching tasks are important for many downstream applications such as bidirectional cross-modal retrieval [23], visual question answering [3], visual navigation [8] and autonomous driving [37].

The vast majority of state-of-the-art visual-language matching methods are in a two-stage manner. In the first stage, a pretrained object detector is used to extract region proposals from images. At the second stage, these proposals are either treated as candidate bounding boxes (bboxes) to be selected from as in instance-level matching (*e.g.*, REG or PG), or regraded as a bottom-up attention mechanism [2] as in image-level matching (*e.g.*, ITM).

Specifically, two-stage instance-level matching methods normally divide the input query into components, ground each component to one proposal and reason about the interactions among them under the guidance of the input query. Take the REG as an example, compared with one-stage grounding methods which regard REG as a generalized object detection (or segmentation) task, two-stage REG methods with the "detect-and-ground" pipeline is more similar to the human way of reasoning. More importantly, it's much easier for two-stage methods to exploit the linguistic structure of referring expressions and perform global reasoning, which is vital when dealing with long, complex expressions. For example in Fig. 1(a), when grounding "*a cat laying down on a white towel next to some keys*", it is even difficult for humans to identify the referent `cat` without considering its contextual objects `towel` and `keys`. Also, it has been pointed out that one-stage methods are insensitive to linguistic variations. When changing the expression in Fig. 1(a) to "*cute cat with stripes looking toward the cat on a white towel*", they tend to refer to the same object (#1) [1]. In general, two-stage methods with perfect proposals (*e.g.*, all human-annotated object regions) can achieve more accurate and explainable grounding results than their one-stage counterparts.

On the other hand, two-stage image-level matching methods cross-match region proposals with query words and use these local matching scores to measure the global image-sentence similarity. For example, it has been widely recognized that by inferring the latent correspondence between each image region and each query word, two-stage ITM methods can better capture the fine-grained interplay between vision and language and are more interpretable to human [38]. As shown in Fig. 1(b), these two images contain overlapping visual content (`monitors`) which makes it difficult to distinguish them from one another on the image level. But by paying attention to other critical objects (*e.g.*, `teddy bear` in the left image, `microphones` in the right image), two-stage methods have a better chance to match them with the right sentence.

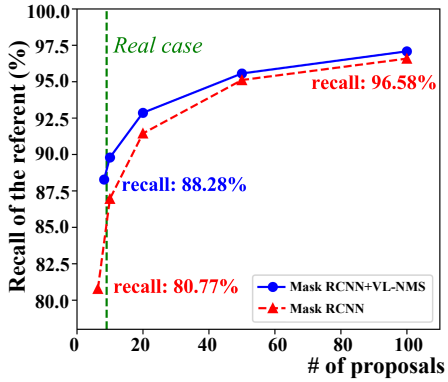

Fig. 2. The recall of the referent (IoU>0.5) vs. number of proposals on the RefCOCO testB set. The real case denotes the actual situation in all state-of-the-art two-stage grounding methods.

R: a **person** holding a slice of **pizza**.

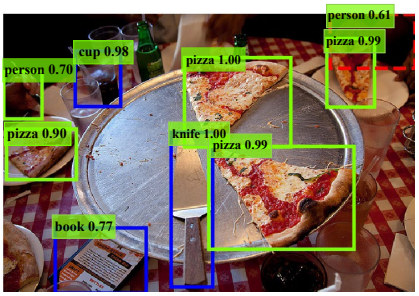

Fig. 3. An example of the first-stage proposals of prevailing MAttNet [85]. The proposals only contain bboxes with high detection confidence regardless of the content of expression (*e.g.*, The candidates knife, book, and cup are not mentioned in expression). The bbox in red dashed line denotes the missing referent.

However, the performance of two-stage visual-language matching methods is heavily bounded by the proposal quality. Especially for REG, when changing the proposals from human-annotated regions to detected regions of a pretrained detector, two-stage REG methods' performance drops dramatically. In this paper, we argue that this huge performance gap between the detected and ground-truth proposals is mainly caused by the **mismatch** between the roles of proposals in the two stages: *the first-stage network generates proposals solely based on detection confidence, while the second-stage network just assumes that the generated proposals will contain all instances mentioned in the text query*. Take REG as an example. For each image, a well pre-trained detector can detect hundreds of detections with a near-perfect recall of the referent and contextual objects (*e.g.*, as shown in Fig. 2, recall of the referent can reach up to 96.58% with top-100 detections). However, to relieve the burden of the referent grounding step in the second stage, current two-stage methods always filter proposals simply based on their detection confidences. These heuristic rules result in a sharp reduction of the recall (*e.g.*, decrease to 80.77% as in Fig. 2), and bring in the mismatch negligently. To illustrate this further, we show a concrete example in Fig. 3. To ground the referent at the second stage, we hope that the proposals contain the referent `person` and its contextual object `pizza`. In contrast, the first-stage network only keeps bboxes with high detection confidence (*e.g.*, `knife`, book, and cup) as proposals, but misses the critical referent `person` (*i.e.*, the red bbox).

In this paper, we propose a novel algorithm VL-NMS, to rectify the mismatch of detected proposals at the conventional first stage. In particular, for each text query, VL-NMS regards all nouns in

the text query as critical objects, and introduces a lightweight relatedness module to predict a probability score for each proposal to be a critical object. The higher predicted score denotes the higher relevance between a proposal and the text query. Then, we fuse the relatedness scores and classification scores, and adopt the fused scores as the suppression criterion in Non-Maximum Suppression (NMS). After NMS, we can filter out the proposals with little relevance to the text query. Finally, all proposals and the text query are fed into the second-stage grounding or matching network, to obtain the final prediction.

Extensive ablations illustrate the superiority of VL-NMS on these visual-language matching tasks. We demonstrate through experiments that VL-NMS can learn the transferable fine-grained correspondence between visual and language. This characteristic is extremely useful when bbox annotations are absent from the target tasks (*e.g.*, the image-text matching tasks). The contributions and novelty of this work are summarized as follows:

- We are the first to point out the proposal bottlenecks in two-stage visual-language matching methods. By investigating the recall of critical objects, we attribute the degraded performance of two-stage methods to the query-agnostic proposals generated at the first stage.
- We propose a novel algorithm VL-NMS to rectify the mismatch of proposals at the first stage by making the proposals query-aware. We also explore different ways to build pseudo ground-truth for training VL-NMS.
- We demonstrate significant performance gains on three REG benchmarks, one phrase grounding benchmark, and one ITM benchmark. It's worth noting that VL-NMS can be generalized and easily integrated into any state-of-the-art two-stage grounding or matching methods to further boost their performance.
- Our method is efficient, generalizable, and transferable, opening doors for many downstream applications such as multimodal summarization.

Highlight. It is worth noting that this paper is a substantial extension of our previous AAAI conference publication [12]. Compared to the original conference version, this new manuscript has made three main improvements: 1) We explore an alternative way in the relatedness module design based on the multi-modal BERT (dubbed VL-NMS$_{\text{Trans}}$). The results show that the new method further surpasses the original performance. 2) We propose a new approach to build pseudo ground-truth by means of weakly supervised phrase grounding. Training VL-NMS no longer needs bbox annotations from the COCO-detection dataset. 3) We extend VL-NMS to other instance-level matching task phrase grounding and image-level matching task image-text matching. Extensive ablations illustrate the superiority of VL-NMS on different visual-language matching tasks.

2 RELATED WORK

2.1 Referring Expression Grounding

Considering different granularities of localization, there are two types of REG: 1) Referring Expression Comprehension (REC) [29, 41, 86, 87], where the referents are localized by bboxes. 2) Referring Expression Segmentation (RES) [30, 58, 61, 80], where the referents are localized by masks.

2.1.1 Referring Expression Comprehension. The current overwhelming majority of REC methods are in a two-stage manner: proposal generation and referent grounding. To the best of our knowledge, existing two-stage works all focus on the second stage. Specifically, they tend to design a more explainable reasoning process by structural modeling [26, 45, 46, 48, 55, 85], or more effective multi-modal interaction mechanism [67, 76]. However, their performance is strictly limited by the proposals from the first stage. Recently, another emerging direction to solve REC is in a one-stage manner [17, 42, 50, 77, 78]. Although one-stage methods achieve faster inference speed empirically,

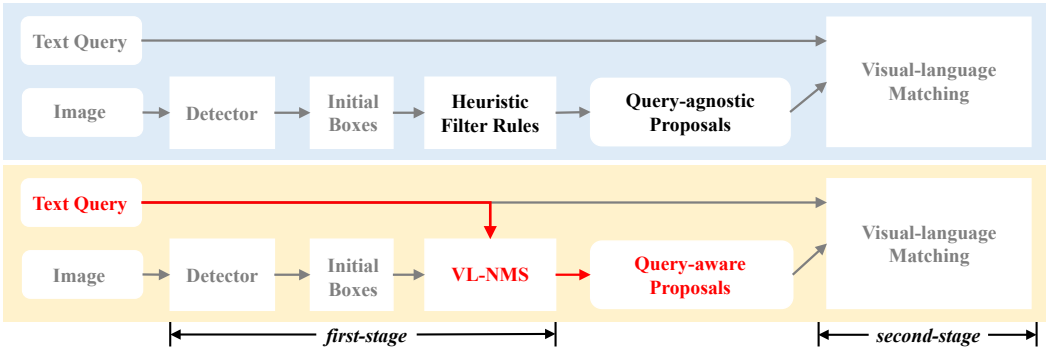

Fig. 4. Upper: A typical two-stage visual-language matching framework, which uses heuristic filter rules to obtain query-agnostic proposals at the first-stage. Below: The VL-NMS module can generate query-aware proposals by considering the text query at the first stage.

they come at a cost of lost interpretability and poor performance in composite expressions. Compared with the one-stage approaches, we both try to achieve text and image communication at an early stage. The difference is that one-stage directly outputs the only referent target, while VL-NMS outputs all objects mentioned in the expression. These query-aware proposals from VL-NMS are closely related to the query (*i.e.*, expression), which can significantly improve both the accuracy and explainability of the second-stage model reasoning. More recently, Transformer has been applied in visual grounding [19, 35, 74, 93] with excellent performance. But there is still the problem of poor interpretability. Besides, the vast majority of methods require a lot of prior knowledge and expertise to design sophisticated networks. This makes them less generalizable. In addition to the methods above, some recently published works [65, 79] are inspired by our previous conference paper. QRNet [79] shares a similar idea with us and tries to resolve the inconsistency in features. But we still have differences, most notably we are based on the two-stage model in order to achieve better interpretability. In this paper, we rectify the overlooked mismatch in two-stage methods and propose VL-NMS. It is worth noting that VL-NMS can be attached on any two-stage model easily and the effect is validated on multiple models and benchmarks.

2.1.2 Referring Expression Segmentation. Unlike REC, most RES works are one-stage methods. They typically utilize a "concatenation-convolution" design to combine the two different modalities: they first concatenate the expression feature with visual features at each location, and then use several conv-layers to fuse the multimodal features for mask generation. To further improve mask qualities, they usually enhance their backbones with more effective features by multi-scale feature fusion [53], feature progressive refinement [6, 32, 40], or novel attention mechanisms [31, 61, 81]. Besides, with the development of two-stage instance segmentation (*e.g.*, Mask R-CNN [25]), two-stage REC methods can be extended to solve RES simply by applying the mask branch upon the predicted bounding box at the end of the second stage. Analogously, VL-NMS can be easily integrated into any two-stage RES method.

2.2 Image-Text Matching

Image-Text matching aims to align images with sentences, normally evaluated by the recall of bidirectional retrieval. Prior works directly learn the global correspondence between images and sentences [22, 69, 72, 92]. These works normally encode images and sentences into holistic feature vectors, project them into a common feature space and try to maximize the similarity between the matched image-sentence pairs. Recent works propose to infer the latent local correspondence

between each image region and each word or noun chunk in the sentence [7, 38, 44]. By exploiting this fine-grained correspondence, the global matching performance can be improved. This type of method typically uses a pretrained object detector to extract region proposals from images, then match them with each word in the sentence. VL-NMS can help to filter out region proposals irrelevant to the sentence and aid the local correspondence inference process.

2.3 Phrase Grounding

Given an image and a sentence, phrase grounding aims to ground all noun phrases in the sentence. There are also two types of solutions: proposal-free methods and proposal-driven methods. Different from REC, the queries in phrase grounding are much simpler, which relieves two-stage methods from complicated relational reasoning and allows them to take more proposals at the second stage[1]. Meanwhile, efforts have been taken to handle the query diversity at the first stage by either using an object detector pre-trained on another large-scale dataset [89] or re-generate proposals with respect to queries and mentioned objects [10]. Recently, a large proportion of phrase grounding works turn to the weakly supervised setting where only image-sentence alignment is provided as annotation [9, 18]. In this paper, we use weakly supervised phrase grounding as an alternative way to capture the cross-modal context in generated region proposals. Besides, VL-NMS is model-agnostic and thus can help various two-stage methods get better performance on phrase grounding.

2.4 Non-Maximum Suppression

Non-Maximum Suppression (NMS) is a de facto standard post-processing step adopted by numerous modern object detectors, which removes duplicate bboxes based on detection confidence. Except for the most prevalent GreedyNMS, multiple improved variants have been proposed recently. Generally, they can be categorized into three groups: 1) Criterion-based [33, 62, 63, 73]: they utilize other scores instead of classification confidence as the criterion to remove bboxes by NMS, *e.g.*, IoU scores. 2) Learning-based [27, 28]: they directly learn an extra network to remove duplicate bboxes. 3) Heuristic-based [4, 47]: they dynamically adjust the thresholds for suppression according to some heuristic rules. In this paper, we are inspired by the criterion-based NMS, and design the VL-NMS, which uses both expression relatedness and detection confidence as the criterion.

3 APPROACH

In this section, we first revisit the typical two-stage visual-language matching framework, and then introduce the details about VL-NMS, including the relatedness module, the ground-truth acquisition, and the training objectives.

3.1 Revisiting Two-Stage Visual-language Matching

The two-stage framework is the most prevalent pipeline for visual-language matching tasks. As shown in Fig. 4, it consists of two separate stages: proposal generation at the first stage and multimodal matching at the second stage.

3.1.1 Proposal Generation. Given an image, current two-stage methods always resort to a well pre-trained detector to obtain a set of initially detected bboxes, and utilize an NMS operation to remove duplicate bboxes. However, even after the NMS operation, there are still thousands of bboxes left (*e.g.*, for the REG task, each image in RefCOCO has an average of 3,500 detections). To relieve the burden of the following multimodal matching step, all existing works further filter these bboxes based on their detection confidences. Although this heuristic filter rule can reduce

[1] At the second stage, REC methods take an average number of 10 proposals while phrase grounding methods can take more than 200 proposals.

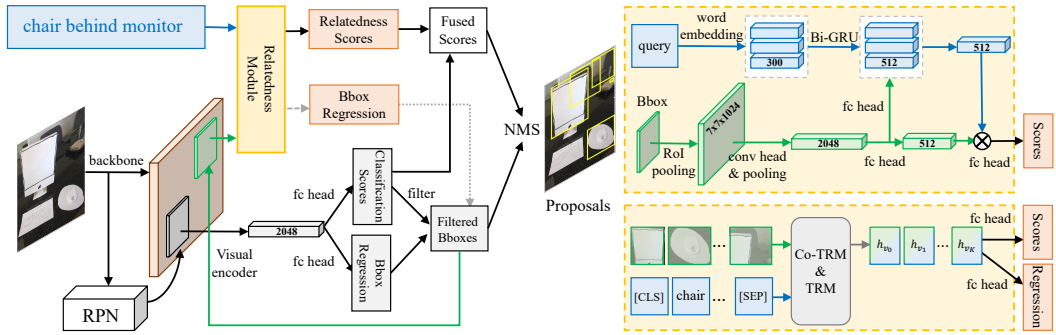

Fig. 5. **Left**: The overview of the VL-NMS model. Given an image, the model uses a pre-trained detector to generate thousands of initial bboxes. Then, the text query and hundreds of filtered bboxes with detection confidence beyond a threshold are fed into the relatedness module to predict the relatedness scores. Lastly, the relatedness scores are fused with detection confidences and the fused scores are used as the suppression criterion of NMS. **Right**: Two types of relatedness module corresponding to VL-NMS$_{\text{FC}}$(top) [12] and VL-NMS$_{\text{Trans}}$(bottom), respectively. We further introduce the regression module in VL-NMS$_{\text{Trans}}$ to improve the quality of bboxes.

the number of proposals, it also results in a drastic drop in the recall of the mentioned instances. Especially for the REG task, this recall drop can be fatal as the grounding process at the second stage will be guaranteed to fail if the referent is missed at the first stage. Detailed recall statistics of the referent and contextual objects on three REG benchmarks are reported in Table 1.

3.1.2 Multimodal Matching. For the REG task, in the training phase, two-stage methods usually use the ground-truth regions in COCO as proposals, and the number is quite small (*e.g.*, each image in RefCOCO has an average of 9.84 ground-truth regions). For explainable grounding, state-of-the-art two-stage grounding methods always compose these proposals into graph [67, 75] or tree [26, 45] structures. As the number of proposals increases linearly, the number of computations increases exponentially. Therefore, in the test phase, it is a must for them to filter detections at the end of the first stage. For the ITM task, in both training and test phases, two-stage methods [7, 38, 44] normally utilize the bottom-up attention mechanism proposed in [2] and take a fixed number of proposals as input at the second stage (normally 36 bboxes per image). Although this number is relatively large compared to REG, reducing the number of proposals can help improve the efficiency of the following image-sentence matching process and greatly shorten the retrieval time.

3.2 Relatedness Module

An overview of the VL-NMS model is shown in Fig. 5. The core of VL-NMS is the relatedness module. We proposed two variants of VL-NMS: a fully-connected layer based VL-NMS$_{\text{FC}}$ and a Transformer-based VL-NMS (VL-NMS$_{\text{Trans}}$). We illustrate the two variants of VL-NMS in Fig. 5.

3.2.1 VL-NMS$_{FC}$. Given an image, a pre-trained detector can generate thousands of initial bboxes. To reduce the computation of the relatedness module, we first use a threshold δ to filter the bboxes with classification confidence, and obtain a filtered bbox set $\mathcal{B}$. For each bbox $\boldsymbol{b}_i \in \mathcal{B}$, we use a region visual encoder e_v (*i.e.*, an RoI Pooling layer and a convolutional head network) to extract the bbox feature $\boldsymbol{v}_i \in \mathbb{R}^v$. Meanwhile, for the text query Q, we use an text encoder e_q (*i.e.*, a Bi-GRU or BERT) to output a set of word features $\{\boldsymbol{w}_1, ..., \boldsymbol{w}_{|Q|}\}$, where $\boldsymbol{w}_j \in \mathbb{R}^q$ is the j-th word feature. For

each bbox $\boldsymbol{b}_i$, we use a soft-attention mechanism [14] to calculate a unique query feature $\boldsymbol{q}_i$ by:

$$\begin{aligned} \boldsymbol{v}_i^a &= \mathrm{MLP}_a(\boldsymbol{v}_i), \quad a_{ij} = \mathrm{FC}_s([\boldsymbol{v}_i^a; \boldsymbol{w}_j]), \\ \alpha_{ij} &= \mathrm{softmax}_j(a_{ij}), \quad \boldsymbol{q}_i = \textstyle\sum_j \alpha_{ij} \boldsymbol{w}_j, \end{aligned} \tag{1}$$

where MLP_a is a two-layer MLP mapping $\boldsymbol{v}_i \in \mathbb{R}^v$ to $\boldsymbol{v}_i^a \in \mathbb{R}^q$, FC_s is a FC layer to calculate the similarity between bbox feature $\boldsymbol{v}_i^a$ and word feature $\boldsymbol{w}_j$, and $[;]$ is a concatenation operation. Then, we combine the features from both modalities and predict the relatedness score r_i:

$$\begin{aligned} \boldsymbol{v}_i^b &= \mathrm{MLP}_b(\boldsymbol{v}_i), \quad \boldsymbol{m}_i = \mathrm{L2Norm}(\boldsymbol{v}_i^b \odot \boldsymbol{q}_i), \\ \hat{r}_i &= \mathrm{FC}_r(\boldsymbol{m}_i), \quad r_i = \mathrm{sigmoid}(\hat{r}_i), \end{aligned} \tag{2}$$

where MLP_b is a two-layer MLP mapping $\boldsymbol{v}_i \in \mathbb{R}^v$ to $\boldsymbol{v}_i^b \in \mathbb{R}^q$, $\odot$ is element-wise multiplication, L2Norm is l_2 normalization, and FC_r is a FC layer mapping $\boldsymbol{m}_i \in \mathbb{R}^q$ to $\hat{r}_i \in \mathbb{R}$.

3.2.2 VL-NMS$_{Trans}$. As show in Fig. 5, VL-NMS$_{\mathrm{Trans}}$ is built on top of the multi-modal BERT [49], which consists of a series of Transformer blocks and co-attention layers. Considering computation and inference time, we implement a shallow, lightweight but efficient version. For the given image, we first get the bboxes feature in the same way as VL-NMS$_{\mathrm{FC}}$. We also encode spatial locations into a 5-d vector (normalized top-left and bottom-right coordinates, and the proportion of the region to total image area). After being projected to the same dimension, the spatial location and visual feature are summed to get the representation of visual tokens. For text query Q, we first convert it to tokens by the tokenization step [20], then put special [CLS] and [SEP] tokens at the beginning and end of the word tokens, respectively. The final text representation is the sum of a token-specific learned embedding [68], position embedding and segment embedding. Therefore, given the image and text query, we can get the visual tokens $\{\tilde{\boldsymbol{v}}_1, \ldots, \tilde{\boldsymbol{v}}_K\}$ and textual tokens $\{[\mathrm{CLS}], \tilde{\boldsymbol{w}}_1, \ldots, \tilde{\boldsymbol{w}}_{|Q|}, [\mathrm{SEP}]\}$ through visual and text encoder respectively, where K is the number of viusal tokens. The input token sequence is $\{\tilde{\boldsymbol{v}}_1, \ldots, \tilde{\boldsymbol{v}}_K, [\mathrm{CLS}], \tilde{\boldsymbol{w}}_1, \ldots, \tilde{\boldsymbol{w}}_{|Q|}, [\mathrm{SEP}]\}$, which can be obtained by concatenating visual tokens and textual tokens. The multi-modal feature then could be fused via a two-layer Transformer and co-attention network, and the output sequences for visual and textual tokens are $\{\boldsymbol{h}_{\tilde{v}_1}, \ldots, \boldsymbol{h}_{\tilde{v}_K}\}$ and $\{\boldsymbol{h}_{\tilde{w}_1}, \ldots, \boldsymbol{h}_{\tilde{w}_{|Q|}}\}$, respectively. To refine the bbox, we further attach a regression module to each visual token $\boldsymbol{h}_{\tilde{v}_i}$.

$$r_i = \mathrm{sigmoid}(\mathrm{FC}(h_{\tilde{v}_i})), \quad t_i = \mathrm{MLP}_t(h_{\tilde{v}_i}), \tag{3}$$

where MLP_t is composed of two ReLU layers and a linear layer. FC layer maps the $h_{\tilde{v}_i}$ to a scalar. r_i and $t_i = (t_i^x, t_i^y, t_i^w, t_i^h)$ denote the prediction of relatedness score and bbox offsets respectively.

After obtaining the relatedness score r_i for bbox $\boldsymbol{b}_i$, we multiply r_i with the classification confidence c_i for bbox $\boldsymbol{b}_i$ from the original detector, and utilize the product of two scores s_i as the suppression criterion of the NMS operation, *i.e.*, $s_i = r_i \times c_i$. We argue that fusing by multiplication is straightforward, doesn't introduce any extra hyper-parameters, and yields competing empirical results over other methods, such as weighted summarization.

Highlight. Inspired by the success of Transformer [64] in different vision tasks, we introduce an advanced VL-NMS$_{\mathrm{Trans}}$ based on the Transformer in this new manuscript. The self-attention mechanism in VL-NMS$_{\mathrm{Trans}}$ inherently helps to find the latent correspondences between visual regions and words. Further, we utilize a regression module to improve the lack of accuracy of bboxes. The more precise bboxes help the two-stage grounding methods achieve better performance.

3.3 Acquisition of Ground-Truth Annotations

To learn the relatedness score for each bbox, we need the ground-truth annotations for all instances mentioned in the text query. However, except for the PG datasets, both REG and ITM datasets don't contain such dense instance-level annotations, making it necessary to build pseudo ground-truth.

For the REG task, current datasets only have annotations about the referent. Thus, we need to generate pseudo ground-truths for contextual objects. Specifically, we explore two alternatives:

- **Text Similarity based Method.** We first assign POS tags to each word using the spaCy POS tagger and extract all nouns in the expression. Then, we calculate the cosine similarity between GloVe embeddings of extracted nouns and category names of ground-truth regions in COCO[2]. Lastly, we use threshold γ to filter regions as the pseudo ground-truths.
- **WSPG based Method.** To relieve two-stage REG methods from depending on COCO detection annotations, we propose to use a weakly supervised phrase grounding (WSPG) method to generate pseudo ground-truth for contextual objects. Note that the performance of WSPG methods is far from ideal. Hence directly using the results of a WSPG model as the first stage proposals is not feasible.

In the training phase, we regard all the pseudo ground-truth bboxes and annotated referent bboxes as foreground bboxes.

For the ITM task, we can use annotations from phrase grounding datasets as our "golden" pseudo ground-truth. Alternatively, to relieve VL-NMS from using extra annotations from other tasks, we propose to transfer the VL-NMS model pretrained on the REG dataset to the ITM task at inference time. Detailed measures and empirical results are described in the experiment section.

Highlight. The three prevalent REG datasets (RefCOCO/RefCOCO+/RefCOCOg) [51, 86] are all build upon the COCO dataset. Therefore, either explicitly or implicitly, most state-of-the-art grounding methods make use of extra COCO annotations. To get rid of the reliance on extra COCO annotations, we propose an alternative way to build pseudo ground-truth. With the WSPG based method, extra COCO annotations are no longer necessary for training VL-NMS.

3.4 Training Objectives for VL-NMS

We explored two types of classification objectives and one regression objective.

3.4.1 Classification objective. **1) Binary XE Loss.** For each bbox $\boldsymbol{b}_i \in \mathcal{B}$, if it has a high overlap (*i.e.*, IoU>0.5) with any foreground bbox, its ground-truth relatedness score r^* is set to 1, otherwise $r^* = 0$. Then the relatedness score prediction becomes a binary classification problem. We can use the binary cross-entropy (XE) loss as the classification objective:

$$L_{\text{cls}} = -\frac{1}{|\mathcal{B}|}\sum_{i=1}^{|\mathcal{B}|} r_i^* \log(r_i) + (1 - r_i^*)\log(1 - r_i). \tag{4}$$

2) Ranking Loss. Generally, if a bbox has a higher IoU with foreground bboxes, the relatedness between the bbox and expression should be higher, *i.e.*, we can use the ranking loss as the training objectives:

$$L_{\text{cls}} = \frac{1}{N}\sum_{(\boldsymbol{b}_i, \boldsymbol{b}_j), \rho_i < \rho_j} \max(0, r_i - r_j + \alpha), \tag{5}$$

where ρ_i denotes the largest IoU value between bbox $\boldsymbol{b}_i$ and foreground bboxes, N is the total number of pos-neg training pairs, and α is a constant to control the ranking margin, set as 0.1. To select the pos-neg pair $(\boldsymbol{b}_i, \boldsymbol{b}_j)$, we follow the sampling-after-splitting strategy [62]. Specifically, we first divide the bbox set $\mathcal{B}$ into 6 subsets based on a quantization q-value: $q_i = \lceil \max(0, \rho_i - 0.5)/0.1 \rceil$,

[2]Two-stage methods always use an object detector pretrained on COCO detection dataset. Thus, we don't use extra or more annotations.

i.e., bboxes with higher IoU values will have larger q-values. Then, all bboxes with $\rho > 0.5$ are selected as positive samples. For each positive sample, we rank all bboxes with smaller q-value based on the predicted relatedness scores and select the top-h bboxes as negative samples.

We empirically find that training with binary XE loss is more robust while training with ranking loss has the advantage of explicitly enforcing ranks within proposals and sometimes yields better results (More results are reported in Sec. 4.1).

3.4.2 Regression Objective. **1) Regression Loss.** In addition to the relatedness score classification loss, we also propose a new regression loss to further improve the proposal quality at the first stage. Specifically, for the bbox regression offsets $t = (t^x, t^y, t^w, t^h)$. We adopt the parameterization [24] for t and obtain the scale-invariant ground-truth $\hat{t} = (\hat{t^x}, \hat{t^y}, \hat{t^w}, \hat{t^h})$. Then we train the regression block with the widely used smooth L1 loss:

$$L_{\text{reg}} = L_{\text{smooth-L1}}(t_i, \hat{t}_i) \tag{6}$$

where $L_{\text{smooth-L1}}$ is the smooth L1 loss.

3.4.3 Overall Training Objective. For VL-NMS$_{\text{FC}}$, either binary XE Loss or ranking Loss are served as the training objective. Since the model with binary XE loss works better, VL-NMS$_{\text{Trans}}$ uses binary XE loss as classification loss. Then, we can train VL-NMS$_{\text{Trans}}$ with the multi-task objective:

$$L = \frac{1}{|\mathcal{B}|}\sum_{i=1}^{|\mathcal{B}|} L_{\text{BXE}}(r_i, r_i^*) + \lambda \frac{1}{N}\sum_{i=1}^{|\mathcal{B}|} r_i^* L_{\text{reg}}(t_i, \hat{t}_i) \tag{7}$$

where L_{BXE} and L_{reg} denote binary cross-entropy loss and smooth L1 loss respectively. λ is a coefficient of L_{reg} to balance these two losses. The L_{reg} is activated only for positive bboxes(*i.e.*, $r_i^* = 1$) and N is the total number of positive bboxes. Although we view the pseudo ground-truths generated by WSPG based Method as foreground bbox, they will not be used to calculate regression loss for the lack of reliable annotations.

Highlight. The previous VL-NMS$_{\text{FC}}$ only uses classification loss to select the objects contained in the query. However, insufficiently precise bboxes can also hinder the subsequent inference steps. To this end, we expect the regression module to enhance the quality of bboxes. Thus, we introduce the smooth L1 loss to train the regression module.

4 EXPERIMENTS

4.1 Results on Referring Expression Grounding

Datasets. We evaluated VL-NMS on three challenging REG benchmarks: 1) **RefCOCO** [86]: It consists of 142,210 referring expressions for 50,000 objects in 19,994 images. These expressions are collected in an interactive game interface [36], and the average length of each expression is 3.5 words. All expression-referent pairs are split into the train, val, testA, and testB sets. The testA set contains images with multiple people and the testB set contains images with multiple objects. 2) **RefCOCO+** [86]: It consists of 141,564 referring expressions for 49,856 objects in 19,992 images. Similar to RefCOCO, these expressions are collected from the same game interface, and have the train, val, testA, and testB splits. But different from RefCOCO, these expressions don't include the absolute location of the referent. 3) **RefCOCOg** [51]: It consists of 104,560 referring expressions for 54,822 objects in 26,711 images. These expressions are collected in a non-interactive way, and the average length of expression is 8.4 words. Compared to RefCOCO and RefCOCO+, expressions in RefCOCOg are more descriptive and involve more objects. We follow the same split as [54].

Evaluation Metrics. We evaluated VL-NMS on two different REG tasks: referring expression comprehension (REC) and referring expression segmentation (RES). For the REC task, we used top-1 accuracy as the evaluation metric. When the IoU between the predicted and ground truth is

Table 1. Recall (%) of the referent and contextual objects. The baseline detector is a ResNet-101 based Mask R-CNN with plain GreedyNMS. 'B' denotes VL-NMS with binary XE loss, 'R' denotes VL-NMS with ranking loss. 'Real' denotes the real case used in the state-of-the-art two-stage methods.

Referent									
	VL-NMS$_{FC}$	RefCOCO			RefCOCO+			RefCOCOg	
		val	testA	testB	val	testA	testB	val	test
N=100		97.60	97.81	96.58	97.79	97.78	96.99	97.18	96.91
	B	97.75	98.59	97.08	97.96	98.39	97.50	97.61	97.44
	R	97.62	98.02	96.78	97.71	98.06	97.14	97.18	97.08
Real		88.84	93.99	80.77	90.71	94.34	84.11	87.83	87.88
	B	**92.51**	**95.56**	**88.28**	**93.42**	**95.86**	**88.95**	**90.28**	**90.34**
	R	90.50	94.75	83.87	91.62	95.14	86.42	89.01	88.96
Contextual Objects									
	VL-NMS$_{FC}$	RefCOCO			RefCOCO+			RefCOCOg	
		val	testA	testB	val	testA	testB	val	test
N=100		90.14	89.85	90.53	89.53	88.47	90.69	90.56	90.30
	B	90.38	90.31	90.64	89.67	88.88	91.04	90.36	90.37
	R	90.22	89.83	90.63	89.70	88.62	90.71	90.67	90.30
Real		74.97	78.60	70.19	76.34	77.45	73.52	75.69	75.87
	B	**78.75**	**80.14**	**76.47**	**78.44**	**78.82**	**77.49**	76.12	76.57
	R	76.79	79.12	72.99	77.66	78.44	75.59	**76.68**	**76.73**

larger than 0.5, the prediction is considered to be correct. For the RES task, we used the overall IoU and Pr@X (the percentage of samples with IoU higher than X)[3] as metrics. Besides, we calculated the average performance on the three benchmarks to show the global performance of the model.

Implementation Details. We built a vocabulary for each dataset by filtering out the words less than 2 times, and exploited the 300-d GloVe embeddings as the initialization of word embeddings. We used an "unk" symbol to replace all words out of the vocabulary. The largest length of sentences was set to 10 for RefCOCO and RefCOCO+, 20 for RefCOCOg. The text encoder e_q is a bidirectional GRU with a hidden size of 256. For the visual encoder e_v, we used the same head network of the Mask R-CNN with ResNet-101 backbone[4] as prior works [85], and utilized the pre-trained weights as initialization. The weights of the original detector (*i.e.*, the gray part in Figure 5) were fixed during training. For VL-NMS$_{Trans}$, the largest length of sentences was doubled and we applied BERT as text encoder following [49]. We used the 2-layer Transformer and co-attention network to provide interaction between two modalities. The whole model was trained with the Adam optimizer. The learning rate was initialized to 4e-4 for the head network, 2e-6 for the relatedness module of VL-NMS$_{Trans}$ and 5e-3 for the rest of network. We used a batch size of 64 for VL-NMS$_{Trans}$ and 8 for VL-NMS$_{FC}$. The thresholds δ and γ were set to 0.05 and 0.4, respectively. For the ranking loss, the top-h was set to 100. We built pseudo ground-truth based on text similarity, if not mentioned otherwise.

4.1.1 Recall Analyses of Critical Objects. To evaluate the effectiveness of the VL-NMS in improving the recall of both referent and contextual objects, we compared VL-NMS with plain GreedyNMS used

[3]Due to the limited space, all RES results with the Pr@X metric are provided in the supplementary materials.
[4]https://github.com/lichengunc/mask-faster-rcnn

Table 2. Performance of VL-NMS on REC and RES with different grounding backbones. The metric is top-1 accuracy (%) for REC and overall IoU (%) for RES. All baselines use the ResNet-101 based Mask R-CNN as first-stage networks. The best and second best methods under each setting are marked in bold and italic fonts, respectively. † denotes the results are from our implementations.

Models	RefCOCO			RefCOCO+			RefCOCOg	
	val	testA	testB	val	testA	testB	val	test
Referring Expression Comprehension								
MAttNet [85]	76.65	81.14	69.99	65.33	71.62	56.02	66.58	67.27
MAttNet†	76.92	81.19	69.58	65.90	*71.53*	57.23	67.52	67.55
+VL-NMS$_{FC}$ B	*78.82*	**82.71**	*73.94*	**66.95**	71.29	*58.40*	*68.89*	*68.67*
+VL-NMS$_{FC}$ R	77.98	82.02	71.64	*66.64*	71.36	58.01	**69.16**	67.63
+VL-NMS$_{Trans}$	**79.16**	*82.31*	**74.52**	66.58	**71.85**	**58.48**	68.87	**68.75**
NMTree [45]	76.41	81.21	70.09	66.46	72.02	57.52	65.87	66.44
NMTree†	76.13	80.17	70.19	66.65	71.48	57.74	65.65	65.94
+VL-NMS$_{FC}$ B	77.39	*81.40*	*72.46*	**67.15**	*71.76*	58.70	*67.30*	**66.93**
+VL-NMS$_{FC}$ R	77.81	**81.69**	71.78	*67.03*	**71.78**	*58.79*	66.81	66.31
+VL-NMS$_{Trans}$	**78.00**	81.09	**72.93**	66.67	71.55	**58.85**	**67.83**	*66.87*
CM-A-E [48]	78.35	83.14	71.32	68.09	73.65	58.03	67.99	68.67
CM-A-E†	78.35	83.12	71.32	68.19	73.04	58.27	69.10	69.20
+VL-NMS$_{FC}$ B	*80.70*	*84.00*	*76.04*	68.25	**73.68**	*59.42*	*70.55*	**70.62**
+VL-NMS$_{FC}$ R	79.55	*83.58*	73.62	*68.51*	73.14	58.38	69.77	70.01
+VL-NMS$_{Trans}$	**80.97**	**84.02**	**76.64**	**68.76**	*73.30*	**60.44**	**70.81**	*70.30*
Referring Expression Segmentation								
MAttNet [85]	56.51	62.37	51.70	46.67	52.39	40.08	47.64	48.61
MAttNet†	57.14	62.34	51.48	47.30	**52.37**	41.14	48.28	49.01
+VL-NMS$_{FC}$ B	**59.75**	**63.48**	*55.66*	**48.39**	51.57	**42.56**	49.54	*50.38*
+VL-NMS$_{FC}$ R	58.32	62.96	53.68	47.87	51.85	41.41	**50.13**	49.07
+VL-NMS$_{Trans}$	*59.73*	*63.43*	**56.44**	*48.32*	*52.00*	*42.27*	*49.81*	**50.67**
NMTree [45]	56.59	63.02	52.06	47.40	53.01	41.56	46.59	47.88
NMTree†	56.78	61.83	52.94	47.75	*52.36*	41.86	46.19	47.41
+VL-NMS$_{FC}$ B	58.35	*62.59*	**55.40**	**48.68**	52.30	*42.64*	*48.14*	*48.59*
+VL-NMS$_{FC}$ R	*58.42*	**62.69**	53.60	48.27	**52.65**	42.18	47.72	48.09
+VL-NMS$_{Trans}$	**59.26**	62.25	*55.00*	*48.31*	52.09	**42.71**	**49.09**	**48.67**
CM-A-E [48]	—	—	—	—	—	—	—	—
CM-A-E†	58.23	64.60	53.14	49.65	**53.90**	41.77	49.10	50.72
+VL-NMS$_{FC}$ B	*61.46*	**65.55**	*57.41*	49.76	*53.84*	*42.66*	*51.21*	**51.90**
+VL-NMS$_{FC}$ R	59.72	64.87	55.63	*49.86*	52.62	41.87	50.13	51.44
+VL-NMS$_{Trans}$	**61.72**	*65.23*	**58.37**	**50.33**	**53.90**	**43.98**	**51.25**	*51.74*

in the baseline detector (*i.e.*, ResNet-101 based Mask R-CNN). Since we only have annotated ground-truth bboxes for the referent, we calculated the recall of pseudo ground-truths to approximate the recall of contextual objects. The results are reported in Table 1, and more detailed results are provided in the supplementary materials. From Table 1, we have the following observations. When using top-100 bboxes as proposals, all three methods can achieve near-perfect recall ($\approx$ 97%) for the referent and acceptable recall ($\approx$ 90%) for the contextual objects, respectively. However, as the number of proposals decreases to a very small number (*e.g.*, $<$ 10 in the real case), the recall of the baseline all drops significantly (*e.g.*, 15.81% for the referent and 20.34% for the contextual objects on

RefCOCO testB). In contrast, VL-NMS can help narrow the gap over all dataset splits. Especially, the improvement is more obvious on the testB set (*e.g.*, 7.51% and 4.85% absolute gains for the recall of referent on RefCOCO and RefCOCO+), where the categories of referents are more diverse and the recalls are relatively lower.

4.1.2 Architecture Agnostic Generalization. Since the VL-NMS model is agnostic to the second stage network, it can be easily integrated into any referent grounding architecture. To evaluate the effectiveness and generalizability of VL-NMS in boosting the performance of different backbones, we incorporated VL-NMS into three state-of-the-art two-stage grounding methods: **MAttNet** [85] , **NMTree** [45], and **CM-A-E** [48]. All results are reported in Table 2. From Table 2, we can observe that all variants of VL-NMS can consistently improve the grounding performance of three backbones on both REC and RES. The improvement is more significant on the testB set (*e.g.*, 5.32% and 5.23% absolute performance gains for CM-A-E in REC and RES), which meets our expectation, *i.e.*, the improvements in the recall of critical objects at the first stage have a strong positive correlation with the improvements of grounding performance at the second stage. Comparing the two variants of VL-NMS, in most of the cases, VL-NMS$_{\text{Trans}}$ achieves better grounding performance.

4.1.3 Comparison with State-of-the-Arts. We incorporate VL-NMS$_{\text{FC}}$ and VL-NMS$_{\text{Trans}}$ into CM-A-E model, dubbed **CM-A-E+VL-NMS$_{\text{FC}}$** and **CM-A-E+VL-NMS$_{\text{Trans}}$**, and compare them against state-of-the-art REC and RES methods. For fair comparison, we group state-of-the-art REC methods into: 1) two-stage methods: **VC** [91], **ParalAttn** [94], **LGRANs** [67], **DGA** [75], **NMTree** [45], **MAttNet** [85], **RvG-Tree** [26], and **CM-A-E** [48]; 2) one-stage methods: **SSG** [17], **FAOA** [78], **RCCF** [42], and **RSC-Large** [77]; 3) Transformer-based methods: **TransVG**[19], **SeqTR**[93], **QR-Net**[79], **VLTVG**[74] and **SiRi**[59]. Analogously, we group state-of-the-art RES methods into: 1) two-stage methods: **MAttNet** [85], **NMTree** [45], and **CM-A-E** [48]; 2) one-stage methods: **STEP** [6], **BRINet** [31], **CMPC** [32], **MCN** [50], **LTS** [34], and **VLT** [21]. The results are reported in Table 3. For the REC task, CM-A-E+VL-NMS achieves a new record-breaking performance that is superior to all existing two-stage REC methods on three benchmarks. Specifically, VL-NMS improves the strong baseline CM-A-E with an average of 2.94%, 0.91%, 2.23% absolute performance gains on RefCOCO, RefCOCO+, and RefCOCOg. For the RES task, CM-A-E+VL-NMS achieves a new state-of-the-art performance of two-stage methods over most of the dataset splits. Similarly, VL-NMS improves CM-A-E with an average of 3.12%. 0.96%, 1.59% absolute performance gains on three benchmarks. Meanwhile, we calculated the mean performance on three benchmarks to intuitively explain the global effect of our method. The results have reported in Table 3, denoted by "*Mean*". It can be seen that the improvement of the new proposed VL-NMS$_{\text{Trans}}$ is approximately the same as that between NMTree and MAttNet, two previous state-of-the-art methods. According to Table 3, Transformer-based models tend to have better performance due to larger parameter sizes and end-to-end training. But in our setting, we focus on comparing two-stage methods because they typically have better interpretability and generalization. Note that since one-stage and two-stage RES models are pretrained on different datasets, the comparison between them is not strictly fair.

4.1.4 Ablation Studies of Pseudo Ground-truth. To validate the effectiveness of pseudo ground-truth, we further compare VL-NMS with a strong baseline: VL-NMS without pseudo ground-truth. The results are shown in Table 4. Both methods are trained with the same set of hyper-parameters and tested with CM-A-E as the grounding backbone. We can observe that VL-NMS performs better on all splits except RefCOCO testB where the performance difference between the two methods is trivial (0.05%). Especially on the RefCOCOg dataset where the expressions are more complex, training with pseudo ground-truth lifts the performance by 1.8%. These results validate the effectiveness of using pseudo ground-truth for contextual objects in the training phase. Meanwhile, from another

Table 3. Comparison with state-of-the-art models on REC and RES. The metric is top-1 accuracy (%) for REC and overall IoU (%) for RES. † denotes the results are from our implementation.

	Models	Backbone	RefCOCO testA	RefCOCO testB	RefCOCO+ testA	RefCOCO+ testB	RefCOCOg test	Mean
Referring Expression Comprehension								
one-s.	SSG [17]	darknet53	76.51	67.50	62.14	49.27	—	—
one-s.	FAOA [78]	darknet53	74.88	66.32	61.89	49.46	58.90	62.29
one-s.	RCCF [42]	dla34	81.06	71.85	70.35	56.32	65.73	69.06
one-s.	RSC-Large [77]	darknet53	80.45	72.30	68.36	67.30	67.20	71.12
transformer	TransVG [19]	res101	83.38	76.94	72.46	59.24	67.98	72.00
transformer	QRNet [79]	Swin-S	85.85	82.34	76.17	63.81	72.52	76.14
transformer	VLTVG [74]	res101	87.24	80.49	78.93	65.17	74.18	77.20
transformer	SeqTR [93]	darknet53	86.51	81.24	76.26	64.88	74.21	76.62
transformer	SiRi [59]	res101	88.56	81.27	82.01	66.33	76.46	78.93
two-s.	VC [91]	vgg16	73.33	67.44	58.40	53.18	—	—
two-s.	ParalAttn [94]	vgg16	75.31	65.52	61.34	50.86	—	—
two-s.	LGRANs [67]	vgg16	76.60	66.40	64.00	53.40	—	—
two-s.	DGA [75]	vgg16	78.42	65.53	69.07	51.99	63.28	65.66
two-s.	NMTree [45]	vgg16	74.81	67.34	61.09	53.45	61.46	63.63
two-s.	MAttNet [85]	res101	81.14	69.99	71.62	56.02	67.27	69.21
two-s.	RvG-Tree [26]	res101	78.61	69.85	67.45	56.66	66.51	67.82
two-s.	NMTree [45]	res101	81.21	70.09	72.02	57.52	66.44	69.45
two-s.	CM-A-E [48]	res101	83.14	71.32	73.65	58.03	68.67	70.96
two-s.	CM-A-E+VL-NMS$_{FC}$	res101	84.00	76.04	**73.68**	59.42	**70.62**	72.75
two-s.	**CM-A-E+VL-NMS$_{Trans}$**	res101	**84.02**	**76.64**	73.30	**60.44**	70.30	**72.94**
Referring Expression Segmentation								
one-s.	STEP [6]	res101	63.46	57.97	52.33	40.41	—	—
one-s.	BRINet [31]	res101	62.99	59.21	52.32	42.41	—	—
one-s.	CMPC [32]	res101	64.53	59.64	53.44	43.23	—	—
one-s.	MCN [50]	darknet53	64.20	59.71	54.99	44.69	49.40	54.60
one-s.	LTS [34]	darknet53	67.76	63.08	58.32	48.02	54.25	58.27
one-s.	VLT [21]	darknet56	68.29	62.73	59.20	49.36	56.65	59.24
two-s.	MAttNet [85]	res101	62.37	51.70	52.39	40.08	48.61	51.03
two-s.	NMTree [45]	res101	63.02	52.06	53.01	41.56	47.88	51.51
two-s.	CM-A-E† [48]	res101	64.60	53.14	**53.90**	41.77	50.72	52.83
two-s.	CM-A-E+VL-NMS$_{FC}$	res101	**65.55**	57.41	53.84	42.66	**51.90**	54.27
two-s.	**CM-A-E+VL-NMS$_{Trans}$**	res101	65.23	**58.37**	**53.90**	**43.98**	51.74	**54.65**

Table 4. Ablation studies of text similarity based pseudo ground-truth on REC task. The grounding backbone is CM-A-E.

VL-NMS	RefCOCO testA	RefCOCO testB	RefCOCO+ testA	RefCOCO+ testB	RefCOCOg test
w/o Pseudo GT	83.63	**76.09**	71.83	58.64	68.76
w/ Pseudo GT	**84.00**	76.04	**73.68**	**59.42**	**70.62**

perspective, VL-NMS trained without pseudo ground-truth can be regarded as a "generalized" one-stage REC model. This suggests that current one-stage REC methods, trained to yield the referent instead of all critical objects, are typically not as qualified as VL-NMS for generating proposals for two-stage REG methods.

4.1.5 Grounding without COCO Annotations. As all three REG benchmarks are built upon the COCO dataset, most state-of-the-art grounding methods, either explicitly or implicitly, make use of extra COCO annotations. Two-stage methods normally use a COCO pretrained detector to extract proposals at the first stage while one-stage methods utilize the pretrained detector weights as initialization of backbone networks. In VL-NMS, we also use COCO annotations to build pseudo ground-truth for contextual objects by the text similarity based method. To relieve the two-stage REG framework from depending on extra data, we attempt to remove COCO detection annotations (*i.e.*, ground-truth bboxes and categories) from the grounding pipeline. During training, we replaced the COCO annotations with the detected bboxes and categories by the widely used Visual Genome pretrained detector [2]. Then, we built pseudo ground-truth for contextual objects in a similar way to text similarity based method. We grounded all noun chunks in the expression, so it can be interpreted as a WSPG method. Then we regarded all pseudo ground-truth bboxes and the annotated referent bbox as foreground bboxes to train VL-NMS. Since only the ground-truth has credible annotations, we merely performed regression on them. Meanwhile, we empirically reduce the weight and label of pseudo ground-truth to 0.5. In the testing phase, we also replace the COCO detector with the Visual Genome detector. The results are shown in Table 5. We can observe that replacing the COCO pretrained detector results in a much inferior grounding performance compared to Table 2 (*e.g.*, performance of CM-A-E decreases by 35.94%). Applying VL-NMS with WSPG-based pseudo ground-truth can consistently and greatly boost the performance of all baselines over three REG benchmarks (*e.g.*, performance of CM-A-E increases by 32.27%, almost as high as the original CM-A-E+VL-NMS in Table 2). We also compared the two ways of generating pseudo ground-truth. As expected, text similarity based method (dubbed VL-NMS (COCO)) generally yields superior results over WSPG based methods (dubbed VL-NMS (WSPG)) by exploiting COCO annotations. The gap is most obvious on RefCOCOg, indicating that it is most sensitive to the quality of the contextual objects. Since its expressions have the longest average lengths and contain the most contextual objects. But the performance gap between these two methods is negligible.

4.1.6 Inference Time of VL-NMS. As VL-NMS needs to forward the detected bboxes of a Mask RCNN back through the RoI pooling layer to calculate the relatedness score, it is reasonable to concern about the added time complexity of VL-NMS. We quantitatively measured the inference time of each component of the two-stage grounding pipeline with VL-NMS. As shown in Table 6, the inference time of VL-NMS is marginal ($\approx$ 16% extra time for both MAttNet and NMTree).

4.2 Results on Phrase Grounding

Datasets. We evaluated VL-NMS on a commonly used phrase grounding benchmark: **Flickr-30K Entities** [57]. It consists of 31,783 images and 427K referred entities. We split 1,000 images for validation, 1,000 images for test, and the rest for training following previous work [89].

Evaluation Metrics. We adopted accuracy as the evaluation metric. The prediction is considered to be correct if the IoU between the prediction and ground truth is larger than 0.5.

Baselines. We applied **DDPN** [89] as the backbone and integrated VL-NMS into it, as DDPN is the state-of-the-art method for two-stage phrase grounding.

su**Results.** Table 7 reports the results of VL-NMS on the Flickr30K Entities test set. Compared with the state-of-the-art two-stage method DDPN, the performance improved by 0.69%, which proves that VL-NMS can be well transferred to the phrase grounding task.

4.3 Results on Image-Text Matching

Datasets. We evaluated VL-NMS on two widely used ITM benchmark: Flickr30K [82] and MS-COCO [43]. Flickr30K consists of 31,000 images collected from Flickr, each associated with five

Table 5. Effectiveness of weakly supervised phrase grounding based pseudo ground-truth on REC task. To avoid using COCO annotations, all baselines use Faster R-CNN pretrained on Visual Genome dataset [2] as first-stage networks. The best and second best methods under each setting are marked in bold and italic fonts, respectively.

Models	RefCOCO		RefCOCO+		RefCOCOg
	testA	testB	testA	testB	test
MAttNet [85]	45.87	51.64	45.60	44.45	45.33
+VL-NMS$_{FC}$ (WSPG)	76.97	68.15	67.95	*55.86*	*64.32*
+VL-NMS$_{Trans}$ (WSPG)	**78.47**	**72.25**	*68.16*	54.90	63.63
+VL-NMS$_{FC}$ (COCO)	*77.92*	*70.70*	**68.93**	**56.33**	**64.85**
NMTree [45]	46.72	51.03	46.02	44.43	44.59
+VL-NMS$_{FC}$ (WSPG)	75.84	66.63	68.37	**55.16**	*63.80*
+VL-NMS$_{Trans}$ (WSPG)	**78.58**	**71.03**	**69.49**	*55.14*	63.38
+VL-NMS$_{FC}$ (COCO)	*77.43*	*69.28*	*69.46*	55.12	**64.26**
CM-A-E [48]	48.06	52.74	48.01	45.76	46.29
+VL-NMS$_{FC}$ (WSPG)	79.28	69.89	69.28	**57.76**	*65.87*
+VL-NMS$_{Trans}$ (WSPG)	**80.33**	**73.03**	**70.31**	*56.31*	65.36
+VL-NMS$_{FC}$ (COCO)	*80.06*	*72.68*	*70.24*	56.29	**66.03**

Table 6. Inference time (seconds) of two-stage grounding pipeline with VL-NMS. Measured on a single NVIDIA 1080Ti.

First Stage		Second Stage	
Res101-MRCNN	**VL-NMS$_{FC}$**	MAttNet	NMTree
0.1893	0.0974	0.4002	0.4058

Table 7. Performance of VL-NMS$_{FC}$ and VL-NMS$_{Trans}$ on phrase grounding. the metric is top-1 accuracy (%). the best methods are marked in bold.

	Models	Accuracy(%)
one-s.	ZSGNet [60]	63.39
	FAOA [78]	68.71
	RSC-Large [77]	69.28
two-s.	Similarity Net [66]	60.89
	CITE [56]	61.33
	DDPN [89]	73.30
	DDPN+VL-NMS$_{FC}$	73.59
	DDPN+VL-NMS$_{Trans}$	**73.99**

human-annotated captions. Following the split in [38], we used 1,000 images for validation, 1,000 images for test, and the rest for training. MS-COCO contains 123,287 images, and each image contains five captions. We follow the split in [38] and use 113,287 images for training, 5,000 images for validation and another 5,000 images for testing.

Evaluation Metrics. Following [38], we adopted Recall@K (R@K) to measure the performance of bidirectional retrieval, namely retrieving sentence with image query (sentence retrieval) and retrieving image with sentence query (image retrieval). R@K is defined as the fraction of queries for which the correct item is retrieved in the top-k scoring items. Also, to evaluate the overall retrieval performance, we report the R@Sum metric which is the sum of all R@K metrics as in [7].

Settings. To train VL-NMS, we need bbox annotations for all critical objects mentioned by the text query. However, ITM datasets don't provide such instance-level annotations. To address this

Table 8. Performance of VL-NMS on ITM task with different matching backbones on Flickr30K. The metrics are Recall@K (%) and Recall@Sum(%). The best and second best methods under each setting are marked in bold and italic fonts, respectively.

	Models	Sentence Retrieval			Image Retrieval			R@sum
		R@1	R@5	R@10	R@1	R@5	R@10	
N=10	SCAN [38]	57.8	83.1	90.1	40.8	68.6	78.1	418.5
	+VL-NMS$_{FC}$ (GT)	*65.4*	*86.6*	*91.9*	*42.9*	*71.0*	*79.7*	*437.5*
	+VL-NMS$_{FC}$ (Transfer)	61.1	86.6	91.5	41.7	70.5	**79.8**	431.2
	+VL-NMS$_{Trans}$ (GT)	**68.1**	**88.9**	**93.4**	**46.7**	**71.3**	79.1	**447.5**
	IMRAM [7]	49.8	78.3	87.5	34.2	62.9	72.9	385.6
	+VL-NMS$_{FC}$ (GT)	*67.8*	*87.6*	*93.0*	*44.5*	**71.7**	*80.1*	*444.7*
	+VL-NMS$_{FC}$ (Transfer)	59.9	85.2	91.2	42.8	*71.5*	**80.6**	431.2
	+VL-NMS$_{Trans}$ (GT)	**72.1**	**90.9**	**95.0**	**45.8**	69.8	78.0	**451.6**

Table 9. Performance of VL-NMS on ITM task with different matching backbones on MS-COCO. The metrics are Recall@K (%) and Recall@Sum(%). The best and second best methods under each setting are marked in bold and italic fonts, respectively.

	Models	Sentence Retrieval			Image Retrieval			R@sum
		R@1	R@5	R@10	R@1	R@5	R@10	
	1K Test Images							
N=10	SCAN [38]	*47.5*	*77.3*	*87.0*	34.7	69.7	81.4	397.6
	+VL-NMS$_{FC}$ (GT)	46.2	75.6	85.9	*37.3*	*72.4*	83.3	*400.7*
	+VL-NMS$_{FC}$ (Transfer)	45.7	76.5	86.4	35.7	71.2	*83.4*	398.8
	+VL-NMS$_{Trans}$ (GT)	**49.8**	**80.2**	**88.5**	**39.5**	**73.8**	**85.6**	**417.4**
	IMRAM [7]	41.9	70.9	80.9	18.3	50.3	63.3	325.6
	+VL-NMS$_{FC}$ (GT)	*46.9*	*75.4*	*86.5*	**32.2**	*63.9*	**76.2**	*381.2*
	+VL-NMS$_{FC}$ (Transfer)	44.7	76.7	86.3	30.9	62.2	75.1	375.9
	+VL-NMS$_{Trans}$ (GT)	**49.8**	**78.1**	**87.3**	*31.7*	**64.0**	**76.2**	**387.2**
	5K Test Images							
N=10	SCAN [38]	*24.8*	*49.9*	*62.0*	16.5	40.0	53.3	246.4
	+VL-NMS$_{FC}$ (GT)	24.2	48.6	61.2	*18.3*	*43.1*	*56.1*	*251.5*
	+VL-NMS$_{FC}$ (Transfer)	22.5	47.6	61.2	17.4	41.5	54.8	245.1
	+VL-NMS$_{Trans}$ (GT)	**28.2**	**53.9**	**65.8**	**19.6**	**44.9**	**58.2**	**270.6**
	IMRAM [7]	21.4	45.1	57.1	10.1	25.5	34.7	193.9
	+VL-NMS$_{FC}$ (GT)	*23.4*	*49.6*	*62.2*	*14.9*	*36.0*	*47.9*	*234.0*
	+VL-NMS$_{FC}$ (Transfer)	21.7	47.5	60.8	13.6	33.6	45.3	222.4
	+VL-NMS$_{Trans}$ (GT)	**26.2**	**52.6**	**64.9**	**15.0**	**36.7**	**48.9**	**244.4**

issue, we explored two alternatives: *1) By using extra annotations (VL-NMS (GT)):* For Flickr30K, we borrowed bbox annotations from Flickr30K Entities, which is a phrase grounding dataset built upon Flickr30K, as golden ground-truth for critical objects. For MS-COCO, we used the annotations for object detection to find caption-related objects. This can serve as the performance upper bound for VL-NMS on ITM task. *2) By means of transfer learning (VL-NMS (Transfer)):* Given image-sentence pairs from the ITM dataset, we directly used a VL-NMS model trained on the REG dataset to generate proposals at the first stage. Specifically, we chose RefCOCOg as the source dataset as it contains longer expressions which is closer to the captions in Flickr30K and MS-COCO. We made this attempt in the belief that the fine-grained correspondence between image regions and text

words learned by VL-NMS is fundamental and hence transferable. We experimented with using 10 proposals at the second stage, for reducing computation time and memory usage during inference.

Baselines. We incorporated VL-NMS into two state-of-the-art two-stage ITM methods: **SCAN** [38] and **IMRAM** [7]. Specifically, we used the SCAN i-t AVG model with the default configuration and Full-IMRAM with a single matching step due to memory constraints.

Results. As is shown in Table 8 and Table 9, all three methods can consistently improve the matching performance. VL-NMS$_{\text{Trans}}$ (GT) generally has higher performance improvements. We attribute it to the annotations of critical objects and performing the regression during training. It can be seen that reducing the number of proposals has a greater impact on the MS-COCO, since it generally has more caption-related objects (5 targets per sentence on average, while Flickr30K is 4.5 in our experiment). For SCAN, by integrating VL-NMS, using fewer proposals (*e.g.*, 10 proposals) can achieve a close and even better performance than the original SCAN (36 proposals per image) on Flickr30K. For IMRAM, the performance drops drastically when reducing the number of proposals to 10. The results are worse than SCAN, suggesting that complex ITM methods are more sensitive to inferior proposals. Applying all three versions of VL-NMS can help capture meaningful visual context with a limited number of proposals, resulting in a huge performance boost over baseline (+59.1% for VL-NMS$_{\text{FC}}$ (GT) and +45.6% for VL-NMS$_{\text{FC}}$ (Transfer) and +66.0% for VL-NMS$_{\text{Trans}}$ (GT) on R@sum metric on Flickr30K, +55.6% for VL-NMS$_{\text{FC}}$ (GT) and +50.3% for VL-NMS$_{\text{FC}}$ (Transfer) and +61.6% for VL-NMS$_{\text{Trans}}$ (GT) on R@sum metric on MS-COCO).

4.4 Qualitative Results

We illustrate the qualitative results between CM-A-E+VL-NMS and baseline CM-A-E on REC and RES tasks in Figure 6. From the results in line (b), we can observe that VL-NMS can assign high attention weights to words that are more relevant to individual referents (*e.g.*, umbrella, man, and zebra). The results in line (c) show that the generated pseudo ground-truth bboxes can almost contain all contextual objects in the expression, except a few objects whose categories are far different from the categories of COCO (*e.g.*, sweater, armrest, and grass). By comparing the results between line (d) and line (f), we have the following observations: 1) The baseline method tends to detect more false-positive proposals (*i.e.*, the blue bboxes), and misses some critical objects (*i.e.*, the red and green bboxes). Instead, VL-NMS can generate expression-aware proposals which are more relevant to the expression. 2) Even for the failure cases of CM-A-E+VL-NMS (*i.e.*, the last two columns), VL-NMS still generates more reasonable proposals (*e.g.*, with fewer false positive proposals), and the grounding errors mainly come from the second stage grounding model. The segmentation results of the two methods are shown in line (e) and line (g). We can observe that when extending REC models to the RES task, the quality of the segmentation mask is heavily dependent on the precision of REC predictions. If the REC model can ground the referent precisely with a bbox, the downstream segmentation branch can segment the referent from the bbox almost perfectly. Thus, by lifting the grounding precision of two-stage REC methods, VL-NMS can also help to improve the performance of two-stage RES methods.

5 CONCLUSIONS AND FUTURE WORKS

In this paper, we focused on the two-stage visual-language grounding and matching, and discussed the overlooked mismatch problem between the roles of proposals in different stages. Particularly, we proposed a novel algorithm VL-NMS to calibrate this mismatch. VL-NMS tackles the problem by considering the query at the first stage, and learns a relatedness score between each detected proposal and the query. The product of the relatedness score and classification score serves as the suppression criterion for the NMS operation. Meanwhile, VL-NMS is agnostic to the downstream grounding and matching step, hence can be integrated into any SOTA two-stage grounding and

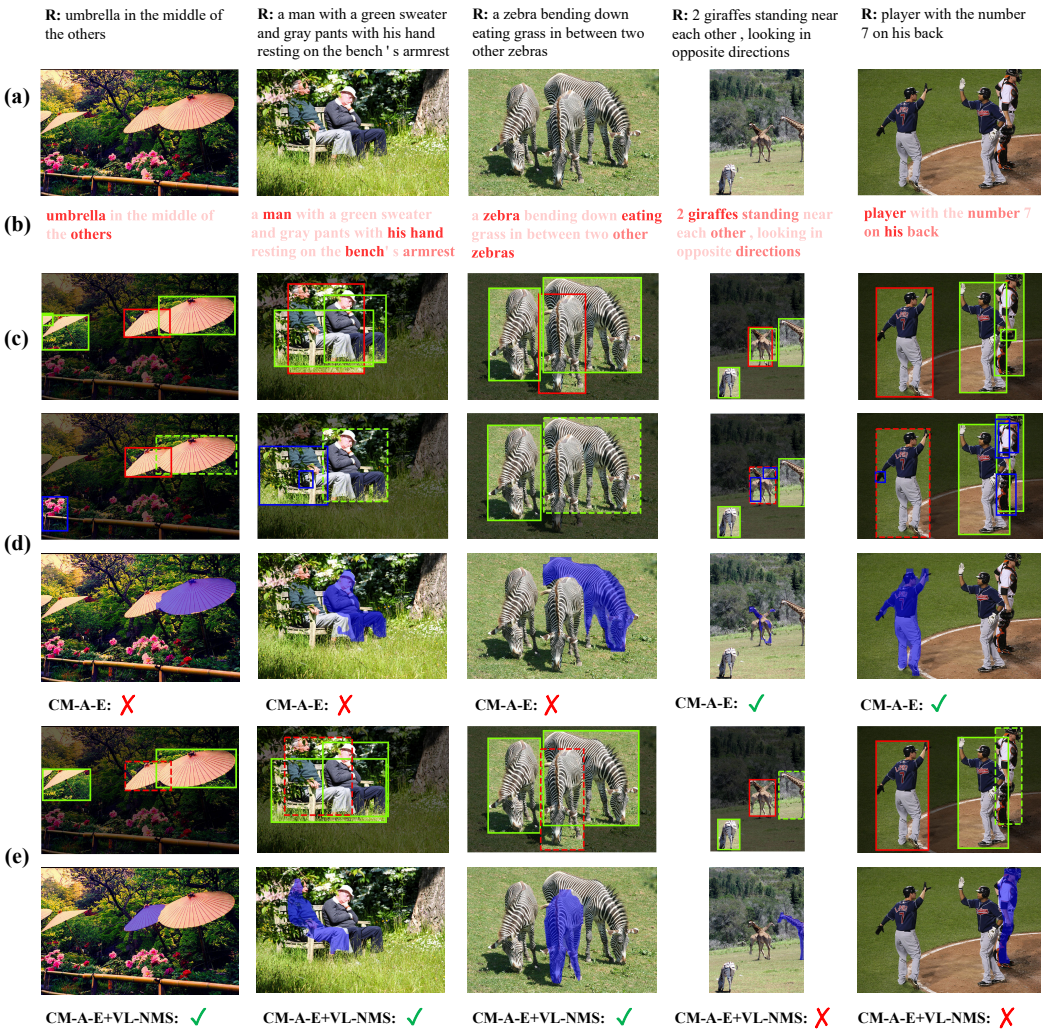

Fig. 6. Qualitative REC and RES results on RefCOCOg showing comparisons between correct (green tick) and wrong referent grounds (red cross) by CM-A-E and CM-A-E+VL-NMS. **(a):** The referring expression and the input image. **(b):** The visualization of word attention weights α (*cf.*, Eq. (1)) for each referent object.**(c):** The annotated ground-truth bbox of the referent (marked in red) and the generated pseudo ground-truth bboxes of the contextual objects (marked in green). **(d):** The upper row demonstrates the proposals generated by an off-the-shelf object detector and the REC predictions of the downstream CM-A-E[48]; the lower row demonstrates the two-stage RES predictions acquired using the REC predictions from the upper row, the detailed method of which is fully described in [85]. **(e):** VL-NMS proposals, the REC and RES predictions from the downstream CM-A-E, arranged in the same format as **(d)**. The predicted bbox in REC is shown in dashed line. The denotations of bbox colors are as follows. **Red:** The bbox hits (IoU>0.5) the ground-truth bbox of the referent; **Green:** The bbox hits one of the pseudo ground-truth bboxes of the contextual objects; **Blue:** The false positive proposals.

matching method. Extensive ablations on various tasks and benchmarks consistently demonstrate that VL-NMS is robust, generalizable, and transferable. Moving forward, we plan to apply VL-NMS

into other proposal-drive visual-language tasks which suffer from the same mismatch issue, *e.g.*, video grounding [5, 11, 70, 71], image captioning [52, 84] and VQA [13, 15, 16, 39, 83, 88, 90].

ACKNOWLEDGMENTS

This work was supported by the National Key Research & Development Project of China (2021ZD0110700), the National Natural Science Foundation of China (U19B2043, 61976185), Zhejiang Innovation Foundation (2019R52002), and the Fundamental Research Funds for the Central Universities (226-2022-00051).

REFERENCES

[1] Arjun R Akula, Spandana Gella, Yaser Al-Onaizan, Song-Chun Zhu, and Siva Reddy. 2020. Words aren't enough, their order matters: On the Robustness of Grounding Visual Referring Expressions. In *arXiv preprint arXiv:2005.01655*.

[2] Peter Anderson, Xiaodong He, Chris Buehler, Damien Teney, Mark Johnson, Stephen Gould, and Lei Zhang. 2018. Bottom-up and top-down attention for image captioning and visual question answering. In *Proceedings of the IEEE/CVF Conference on Computer Vision and Pattern Recognition*.

[3] Stanislaw Antol, Aishwarya Agrawal, Jiasen Lu, Margaret Mitchell, Dhruv Batra, C Lawrence Zitnick, and Devi Parikh. 2015. Vqa: Visual question answering. In *Proceedings of the IEEE International Conference on Computer Vision*.

[4] Navaneeth Bodla, Bharat Singh, Rama Chellappa, and Larry S Davis. 2017. Soft-NMS–improving object detection with one line of code. In *Proceedings of the IEEE International Conference on Computer Vision*.

[5] Meng Cao, Long Chen, Mike Zheng Shou, Can Zhang, and Yuexian Zou. 2021. On pursuit of designing multi-modal transformer for video grounding. In *Conference on Empirical Methods in Natural Language Processing*.

[6] Ding-Jie Chen, Songhao Jia, Yi-Chen Lo, Hwann-Tzong Chen, and Tyng-Luh Liu. 2019. See-through-text grouping for referring image segmentation. In *Proceedings of the IEEE International Conference on Computer Vision*.

[7] Hui Chen, Guiguang Ding, Xudong Liu, Zijia Lin, Ji Liu, and Jungong Han. 2020. Imram: Iterative matching with recurrent attention memory for cross-modal image-text retrieval. In *Proceedings of the IEEE/CVF Conference on Computer Vision and Pattern Recognition*.

[8] Howard Chen, Alane Suhr, Dipendra Misra, Noah Snavely, and Yoav Artzi. 2019. Touchdown: Natural language navigation and spatial reasoning in visual street environments. In *Proceedings of the IEEE/CVF Conference on Computer Vision and Pattern Recognition*.

[9] Kan Chen, Jiyang Gao, and Ram Nevatia. 2018. Knowledge aided consistency for weakly supervised phrase grounding. In *Proceedings of the IEEE/CVF Conference on Computer Vision and Pattern Recognition*.

[10] Kan Chen, Rama Kovvuri, and Ram Nevatia. 2017. Query-guided regression network with context policy for phrase grounding. In *Proceedings of the IEEE International Conference on Computer Vision*.

[11] Long Chen, Chujie Lu, Siliang Tang, Jun Xiao, Dong Zhang, Chilie Tan, and Xiaolin Li. 2020. Rethinking the Bottom-Up Framework for Query-Based Video Localization. In *Proceedings of the AAAI Conference on Artificial Intelligence*.

[12] Long Chen, Wenbo Ma, Jun Xiao, Hanwang Zhang, and Shih-Fu Chang. 2021. Ref-NMS: Breaking Proposal Bottlenecks in Two-Stage Referring Expression Grounding. In *Proceedings of the AAAI Conference on Artificial Intelligence*.

[13] Long Chen, Xin Yan, Jun Xiao, Hanwang Zhang, Shiliang Pu, and Yueting Zhuang. 2020. Counterfactual samples synthesizing for robust visual question answering. In *Proceedings of the IEEE/CVF Conference on Computer Vision and Pattern Recognition*.

[14] Long Chen, Hanwang Zhang, Jun Xiao, Liqiang Nie, Jian Shao, Wei Liu, and Tat-Seng Chua. 2017. Sca-cnn: Spatial and channel-wise attention in convolutional networks for image captioning. In *Proceedings of the IEEE/CVF Conference on Computer Vision and Pattern Recognition*.

[15] Long Chen, Yuhang Zheng, Yulei Niu, Hanwang Zhang, and Jun Xiao. 2021. Counterfactual samples synthesizing and training for robust visual question answering. *arXiv preprint arXiv:2110.01013* (2021).

[16] Long Chen, Yuhang Zheng, and Jun Xiao. 2022. Rethinking data augmentation for robust visual question answering. In *European Conference on Computer Vision*. 95–112.

[17] Xinpeng Chen, Lin Ma, Jingyuan Chen, Zequn Jie, Wei Liu, and Jiebo Luo. 2018. Real-time referring expression comprehension by single-stage grounding network. In *arXiv preprint arXiv:1812.03426*.

[18] Samyak Datta, Karan Sikka, Anirban Roy, Karuna Ahuja, Devi Parikh, and Ajay Divakaran. 2019. Align2ground: Weakly supervised phrase grounding guided by image-caption alignment. In *Proceedings of the IEEE International Conference on Computer Vision*.

[19] Jiajun Deng, Zhengyuan Yang, Tianlang Chen, Wengang Zhou, and Houqiang Li. 2021. Transvg: End-to-end visual grounding with transformers. In *Proceedings of the IEEE/CVF International Conference on Computer Vision*. 1769–1779.

[20] Jacob Devlin, Ming-Wei Chang, Kenton Lee, and Kristina Toutanova. 2018. Bert: Pre-training of deep bidirectional transformers for language understanding. *arXiv preprint arXiv:1810.04805* (2018).

[21] Henghui Ding, Chang Liu, Suchen Wang, and Xudong Jiang. 2021. Vision-language transformer and query generation for referring segmentation. In *Proceedings of the IEEE/CVF International Conference on Computer Vision*. 16321–16330.

[22] Fartash Faghri, David J Fleet, Jamie Ryan Kiros, and Sanja Fidler. 2017. Vse++: Improving visual-semantic embeddings with hard negatives. In *arXiv preprint arXiv:1707.05612*.

[23] Fangxiang Feng, Xiaojie Wang, and Ruifan Li. 2014. Cross-modal retrieval with correspondence autoencoder. In *Proceedings of the 22nd ACM international conference on Multimedia*.

[24] Ross Girshick, Jeff Donahue, Trevor Darrell, and Jitendra Malik. 2014. Rich feature hierarchies for accurate object detection and semantic segmentation. In *Proceedings of the IEEE Conference on Computer Vision and Pattern Recognition*.

[25] Kaiming He, Georgia Gkioxari, Piotr Dollár, and Ross Girshick. 2017. Mask r-cnn. In *Proceedings of the IEEE International Conference on Computer Vision*.

[26] Richang Hong, Daqing Liu, Xiaoyu Mo, Xiangnan He, and Hanwang Zhang. 2019. Learning to compose and reason with language tree structures for visual grounding. In *IEEE Transactions on Pattern Analysis and Machine Intelligence*.

[27] Jan Hosang, Rodrigo Benenson, and Bernt Schiele. 2017. Learning non-maximum suppression. In *Proceedings of the IEEE/CVF Conference on Computer Vision and Pattern Recognition*.

[28] Han Hu, Jiayuan Gu, Zheng Zhang, Jifeng Dai, and Yichen Wei. 2018. Relation networks for object detection. In *Proceedings of the IEEE/CVF Conference on Computer Vision and Pattern Recognition*.

[29] Ronghang Hu, Marcus Rohrbach, Jacob Andreas, Trevor Darrell, and Kate Saenko. 2017. Modeling relationships in referential expressions with compositional modular networks. In *Proceedings of the IEEE/CVF Conference on Computer Vision and Pattern Recognition*.

[30] Ronghang Hu, Marcus Rohrbach, and Trevor Darrell. 2016. Segmentation from natural language expressions. In *European Conference on Computer Vision*.

[31] Zhiwei Hu, Guang Feng, Jiayu Sun, Lihe Zhang, and Huchuan Lu. 2020. Bi-Directional Relationship Inferring Network for Referring Image Segmentation. In *Proceedings of the IEEE/CVF Conference on Computer Vision and Pattern Recognition*.

[32] Shaofei Huang, Tianrui Hui, Si Liu, Guanbin Li, Yunchao Wei, Jizhong Han, Luoqi Liu, and Bo Li. 2020. Referring Image Segmentation via Cross-Modal Progressive Comprehension. In *Proceedings of the IEEE/CVF Conference on Computer Vision and Pattern Recognition*.

[33] Borui Jiang, Ruixuan Luo, Jiayuan Mao, Tete Xiao, and Yuning Jiang. 2018. Acquisition of localization confidence for accurate object detection. In *European Conference on Computer Vision*.

[34] Ya Jing, Tao Kong, Wei Wang, Liang Wang, Lei Li, and Tieniu Tan. 2021. Locate then segment: A strong pipeline for referring image segmentation. In *Proceedings of the IEEE/CVF Conference on Computer Vision and Pattern Recognition*.

[35] Aishwarya Kamath, Mannat Singh, Yann LeCun, Gabriel Synnaeve, Ishan Misra, and Nicolas Carion. 2021. MDETR-modulated detection for end-to-end multi-modal understanding. In *Proceedings of the IEEE/CVF International Conference on Computer Vision*. 1780–1790.

[36] Sahar Kazemzadeh, Vicente Ordonez, Mark Matten, and Tamara Berg. 2014. Referitgame: Referring to objects in photographs of natural scenes. In *Proceedings of the 2014 conference on empirical methods in natural language processing*.

[37] Jinkyu Kim, Teruhisa Misu, Yi-Ting Chen, Ashish Tawari, and John Canny. 2019. Grounding human-to-vehicle advice for self-driving vehicles. In *Proceedings of the IEEE/CVF Conference on Computer Vision and Pattern Recognition*.

[38] Kuang-Huei Lee, Xi Chen, Gang Hua, Houdong Hu, and Xiaodong He. 2018. Stacked cross attention for image-text matching. In *European Conference on Computer Vision*.

[39] Qun Li, Fu Xiao, Le An, Xianzhong Long, and Xiaochuan Sun. 2019. Semantic concept network and deep walk-based visual question answering. *ACM Transactions on Multimedia Computing, Communications, and Applications* (2019).

[40] Ruiyu Li, Kaican Li, Yi-Chun Kuo, Michelle Shu, Xiaojuan Qi, Xiaoyong Shen, and Jiaya Jia. 2018. Referring image segmentation via recurrent refinement networks. In *Proceedings of the IEEE/CVF Conference on Computer Vision and Pattern Recognition*.

[41] Xiangyang Li and Shuqiang Jiang. 2018. Bundled Object Context for Referring Expressions. *IEEE Transactions on Multimedia (TMM)* (2018), 2749–2760.

[42] Yue Liao, Si Liu, Guanbin Li, Fei Wang, Yanjie Chen, Chen Qian, and Bo Li. 2020. A Real-Time Cross-modality Correlation Filtering Method for Referring Expression Comprehension. In *Proceedings of the IEEE/CVF Conference on Computer Vision and Pattern Recognition*.

[43] Tsung-Yi Lin, Michael Maire, Serge Belongie, James Hays, Pietro Perona, Deva Ramanan, Piotr Dollár, and C Lawrence Zitnick. 2014. Microsoft coco: Common objects in context. In *European conference on computer vision*.

[44] Chunxiao Liu, Zhendong Mao, Tianzhu Zhang, Hongtao Xie, Bin Wang, and Yongdong Zhang. 2020. Graph structured network for image-text matching. In *Proceedings of the IEEE/CVF Conference on Computer Vision and Pattern Recognition*.

[45] Daqing Liu, Hanwang Zhang, Feng Wu, and Zheng-Jun Zha. 2019. Learning to assemble neural module tree networks for visual grounding. In *Proceedings of the IEEE International Conference on Computer Vision*.

[46] Daqing Liu, Hanwang Zhang, Zheng-Jun Zha, Meng Wang, and Qianru Sun. 2019. Joint Visual Grounding with Language Scene Graphs. In *arXiv preprint arXiv:1906.03561*.

[47] Songtao Liu, Di Huang, and Yunhong Wang. 2019. Adaptive nms: Refining pedestrian detection in a crowd. In *Proceedings of the IEEE/CVF Conference on Computer Vision and Pattern Recognition*.

[48] Xihui Liu, Zihao Wang, Jing Shao, Xiaogang Wang, and Hongsheng Li. 2019. Improving referring expression grounding with cross-modal attention-guided erasing. In *Proceedings of the IEEE/CVF Conference on Computer Vision and Pattern Recognition*.

[49] Jiasen Lu, Dhruv Batra, Devi Parikh, and Stefan Lee. 2019. Vilbert: Pretraining task-agnostic visiolinguistic representations for vision-and-language tasks. *Advances in Neural Information Processing Systems* (2019).

[50] Gen Luo, Yiyi Zhou, Xiaoshuai Sun, Liujuan Cao, Chenglin Wu, Cheng Deng, and Rongrong Ji. 2020. Multi-task Collaborative Network for Joint Referring Expression Comprehension and Segmentation. In *Proceedings of the IEEE/CVF Conference on Computer Vision and Pattern Recognition*.

[51] Junhua Mao, Jonathan Huang, Alexander Toshev, Oana Camburu, Alan L Yuille, and Kevin Murphy. 2016. Generation and comprehension of unambiguous object descriptions. In *Proceedings of the IEEE/CVF Conference on Computer Vision and Pattern Recognition*.

[52] Yangjun Mao, Long Chen, Zhihong Jiang, Dong Zhang, Zhimeng Zhang, Jian Shao, and Jun Xiao. 2022. Rethinking the reference-based distinctive image captioning. In *Proceedings of the 30th ACM International Conference on Multimedia*. 4374–4384.

[53] Edgar Margffoy-Tuay, Juan C Pérez, Emilio Botero, and Pablo Arbeláez. 2018. Dynamic multimodal instance segmentation guided by natural language queries. In *European Conference on Computer Vision*.

[54] Varun K Nagaraja, Vlad I Morariu, and Larry S Davis. 2016. Modeling context between objects for referring expression understanding. In *European Conference on Computer Vision*.

[55] Yulei Niu, Hanwang Zhang, Zhiwu Lu, and Shih-Fu Chang. 2019. Variational Context: Exploiting Visual and Textual Context for Grounding Referring Expressions. *IEEE Transactions on Pattern Analysis and Machine Intelligence* (2019).

[56] Bryan A Plummer, Paige Kordas, M Hadi Kiapour, Shuai Zheng, Robinson Piramuthu, and Svetlana Lazebnik. 2018. Conditional image-text embedding networks. In *Proceedings of the European Conference on Computer Vision*. 249–264.

[57] Bryan A Plummer, Liwei Wang, Chris M Cervantes, Juan C Caicedo, Julia Hockenmaier, and Svetlana Lazebnik. 2015. Flickr30k entities: Collecting region-to-phrase correspondences for richer image-to-sentence models. In *Proceedings of the IEEE International Conference on Computer Vision*. 2641–2649.

[58] Shuang Qiu, Yao Zhao, Jianbo Jiao, Yunchao Wei, and Shikui Wei. 2020. Referring Image Segmentation by Generative Adversarial Learning. *IEEE Transactions on Multimedia (TMM)* (2020).

[59] Mengxue Qu, Yu Wu, Wu Liu, Qiqi Gong, Xiaodan Liang, Olga Russakovsky, Yao Zhao, and Yunchao Wei. 2022. SiRi: A Simple Selective Retraining Mechanism for Transformer-based Visual Grounding. In *arXiv preprint arXiv:2207.13325*.

[60] Arka Sadhu, Kan Chen, and Ram Nevatia. 2019. Zero-shot grounding of objects from natural language queries. In *Proceedings of the IEEE/CVF International Conference on Computer Vision*. 4694–4703.

[61] Hengcan Shi, Hongliang Li, Fanman Meng, and Qingbo Wu. 2018. Key-word-aware network for referring expression image segmentation. In *European Conference on Computer Vision*.

[62] Zhiyu Tan, Xuecheng Nie, Qi Qian, Nan Li, and Hao Li. 2019. Learning to rank proposals for object detection. In *Proceedings of the IEEE International Conference on Computer Vision*.

[63] Lachlan Tychsen-Smith and Lars Petersson. 2018. Improving object localization with fitness nms and bounded iou loss. In *Proceedings of the IEEE/CVF Conference on Computer Vision and Pattern Recognition*.

[64] Ashish Vaswani, Noam Shazeer, Niki Parmar, Jakob Uszkoreit, Llion Jones, Aidan N Gomez, Łukasz Kaiser, and Illia Polosukhin. 2017. Attention is all you need. In *Advances in Neural Information Processing Systems*, Vol. 30.

[65] Guoqing Wang, Chao Yang, Su Feng, and Bin Jiang. 2022. LPGN: Language-Guided Proposal Generation Network for Referring Expression Comprehension. In *2022 IEEE International Conference on Multimedia and Expo*.

[66] Liwei Wang, Yin Li, Jing Huang, and Svetlana Lazebnik. 2018. Learning two-branch neural networks for image-text matching tasks. *IEEE Transactions on Pattern Analysis and Machine Intelligence* (2018), 394–407.

[67] Peng Wang, Qi Wu, Jiewei Cao, Chunhua Shen, Lianli Gao, and Anton van den Hengel. 2019. Neighbourhood watch: Referring expression comprehension via language-guided graph attention networks. In *Proceedings of the IEEE/CVF Conference on Computer Vision and Pattern Recognition*.

[68] Yonghui Wu, Mike Schuster, Zhifeng Chen, Quoc V Le, Mohammad Norouzi, Wolfgang Macherey, Maxim Krikun, Yuan Cao, Qin Gao, Klaus Macherey, et al. 2016. Google's neural machine translation system: Bridging the gap between human and machine translation. *arXiv preprint arXiv:1609.08144* (2016).

[69] Yiling Wu, Shuhui Wang, and Qingming Huang. 2018. Learning semantic structure-preserved embeddings for cross-modal retrieval. In *Proceedings of the 26th ACM international conference on Multimedia*.

[70] Shaoning Xiao, Long Chen, Jian Shao, Yueting Zhuang, and Jun Xiao. 2021. Natural language video localization with learnable moment proposals. In *Conference on Empirical Methods in Natural Language Processing*.

[71] Shaoning Xiao, Long Chen, Songyang Zhang, Wei Ji, Jian Shao, Lu Ye, and Jun Xiao. 2021. Boundary Proposal Network for Two-Stage Natural Language Video Localization. In *Proceedings of the AAAI Conference on Artificial Intelligence*.

[72] Xing Xu, Yifan Wang, Yixuan He, Yang Yang, Alan Hanjalic, and Heng Tao Shen. 2021. Cross-modal hybrid feature fusion for image-sentence matching. *ACM Transactions on Multimedia Computing, Communications, and Applications* (2021), 1–23.

[73] Chenhongyi Yang, Vitaly Ablavsky, Kaihong Wang, Qi Feng, and Margrit Betke. 2019. Learning to Separate: Detecting Heavily-Occluded Objects in Urban Scenes. In *arXiv preprint arXiv:1912.01674*.

[74] Li Yang, Yan Xu, Chunfeng Yuan, Wei Liu, Bing Li, and Weiming Hu. 2022. Improving Visual Grounding with Visual-Linguistic Verification and Iterative Reasoning. In *Proceedings of the IEEE/CVF Conference on Computer Vision and Pattern Recognition*. 9499–9508.

[75] Sibei Yang, Guanbin Li, and Yizhou Yu. 2019. Dynamic graph attention for referring expression comprehension. In *Proceedings of the IEEE International Conference on Computer Vision*.

[76] Sibei Yang, Guanbin Li, and Yizhou Yu. 2020. Graph-Structured Referring Expression Reasoning in The Wild. In *Proceedings of the IEEE/CVF Conference on Computer Vision and Pattern Recognition*.

[77] Zhengyuan Yang, Tianlang Chen, Liwei Wang, and Jiebo Luo. 2020. Improving One-stage Visual Grounding by Recursive Sub-query Construction. In *European Conference on Computer Vision*.

[78] Zhengyuan Yang, Boqing Gong, Liwei Wang, Wenbing Huang, Dong Yu, and Jiebo Luo. 2019. A fast and accurate one-stage approach to visual grounding. In *Proceedings of the IEEE International Conference on Computer Vision*.

[79] Jiabo Ye, Junfeng Tian, Ming Yan, Xiaoshan Yang, Xuwu Wang, Ji Zhang, Liang He, and Xin Lin. 2022. Shifting More Attention to Visual Backbone: Query-modulated Refinement Networks for End-to-End Visual Grounding. In *Proceedings of the IEEE/CVF Conference on Computer Vision and Pattern Recognition*. 15502–15512.

[80] Linwei Ye, Zhi Liu, and Yang Wang. 2020. Dual Convolutional LSTM Network for Referring Image Segmentation. *IEEE Transactions on Multimedia (TMM)* (2020), 3224–3235.

[81] Linwei Ye, Mrigank Rochan, Zhi Liu, and Yang Wang. 2019. Cross-modal self-attention network for referring image segmentation. In *Proceedings of the IEEE/CVF Conference on Computer Vision and Pattern Recognition*.

[82] Peter Young, Alice Lai, Micah Hodosh, and Julia Hockenmaier. 2014. From image descriptions to visual denotations: New similarity metrics for semantic inference over event descriptions. *Transactions of the Association for Computational Linguistics* (2014).

[83] Dongfei Yu, Jianlong Fu, Xinmei Tian, and Tao Mei. 2019. Multi-source multi-level attention networks for visual question answering. *ACM Transactions on Multimedia Computing, Communications, and Applications* (2019), 1–20.

[84] Jun Yu, Jing Li, Zhou Yu, and Qingming Huang. 2019. Multimodal transformer with multi-view visual representation for image captioning. *IEEE transactions on circuits and systems for video technology* (2019), 4467–4480.

[85] Licheng Yu, Zhe Lin, Xiaohui Shen, Jimei Yang, Xin Lu, Mohit Bansal, and Tamara L Berg. 2018. Mattnet: Modular attention network for referring expression comprehension. In *Proceedings of the IEEE/CVF Conference on Computer Vision and Pattern Recognition*.

[86] Licheng Yu, Patrick Poirson, Shan Yang, Alexander C Berg, and Tamara L Berg. 2016. Modeling context in referring expressions. In *European Conference on Computer Vision*.

[87] Licheng Yu, Hao Tan, Mohit Bansal, and Tamara L Berg. 2017. A joint speaker-listener-reinforcer model for referring expressions. In *Proceedings of the IEEE/CVF Conference on Computer Vision and Pattern Recognition*.

[88] Zhou Yu, Jun Yu, Chenchao Xiang, Jianping Fan, and Dacheng Tao. 2018. Beyond bilinear: Generalized multimodal factorized high-order pooling for visual question answering. *IEEE transactions on neural networks and learning systems* (2018), 5947–5959.

[89] Zhou Yu, Jun Yu, Chenchao Xiang, Zhou Zhao, Qi Tian, and Dacheng Tao. 2018. Rethinking diversified and discriminative proposal generation for visual grounding. In *arXiv preprint arXiv:1805.03508*.

[90] Zhou Yu, Zhu Junjie Yu, Jun, and Zhenzhong Kuang. 2022. Knowledge-representation-enhanced multimodal Transformer for scene text visual question answering. *Journal of Image and Graphics* (2022), 2761–2774.

[91] Hanwang Zhang, Yulei Niu, and Shih-Fu Chang. 2018. Grounding referring expressions in images by variational context. In *Proceedings of the IEEE/CVF Conference on Computer Vision and Pattern Recognition*.

[92] Lingling Zhang, Minnan Luo, Jun Liu, Xiaojun Chang, Yi Yang, and Alexander G. Hauptmann. 2020. Deep Top-k Ranking for Image–Sentence Matching. *IEEE Transactions on Multimedia (TMM)* (2020), 775–785.

[93] Chaoyang Zhu, Yiyi Zhou, Yunhang Shen, Gen Luo, Xingjia Pan, Mingbao Lin, Chao Chen, Liujuan Cao, Xiaoshuai Sun, and Rongrong Ji. 2022. SeqTR: A Simple yet Universal Network for Visual Grounding. In *arXiv preprint arXiv:2203.16265*.

[94] Bohan Zhuang, Qi Wu, Chunhua Shen, Ian Reid, and Anton van den Hengel. 2018. Parallel attention: A unified framework for visual object discovery through dialogs and queries. In *Proceedings of the IEEE/CVF Conference on Computer Vision and Pattern Recognition*.